FLEXIBILITY POTENTIAL OF HEAT PUMPS THROUGH DEMAND SIDE MANAGEMENT IN BUILDINGS

Agostino Gambarotta[1,2], Mirko Morini[1,2], Costanza Saletti[1]*

[1]University of Parma, Department of Engineering for Industrial Systems and Technologies (DISTI), Parma, Italy
[2]University of Parma, Center for Energy and Environment (CIDEA), Parma, Italy

*Corresponding Author: costanza.saletti@unipr.it

ABSTRACT

Energy transition is progressively replacing conventional fossil-based energy systems with renewable energy sources, which are by nature not flexible and cannot be managed to meet energy needs. Hence, it is of key importance to have flexibility on the demand side to ensure a balance between energy supply and demand. One possible strategy to achieve this is known as Demand Side Management (DSM), consisting of actively changing user demand to obtain a more efficient system operation. When heat is supplied by heat pumps, and therefore it is tranferred into an electricity demand, DSM allows electricity to be stored as heat within the building thermal mass (e.g. by varying the temperature set-points), in order to reduce the electricity demand in subsequent periods. This study aims to characterize the potential of heat pumps supplying heat to buildings in order to implement this DSM strategy and, therefore, to offer flexibility or balancing services to the power grid. The dynamic behavior of a binary system comprising a building and a heat pump, including the heat distribution circuit for generality, is simulated through a model in MATLAB®/Simulink®. A set of experiments is carried out by preheating the building at different hours of the day (i.e. increasing the comfort set-point) and by sensitivity analyses on the building thermal properties (i.e. time constant). The flexibility potential is assessed by defining and evaluating key performance indicators that represent the behavior of the binary system, e.g. peak energy reduction, amount of electricity used to preheat the building and avoided during its discharge, and building discharge time. The results remark the periods of the day in which it is more effective to apply DSM, leading to a potential electricity saving of up to 5 % thanks to a more efficient operation of the heat pump, when considering its variable performance with the load. The discharge time of the building is also highly variable, ranging from 2 h to 8 h. The analysis of these indicators can open up new management opportunities in communities of buildings.

1 INTRODUCTION

Over the last few decades, the mitigation of climate change through the reduction in greenhouse gas emissions, also referred to as decarbonization, has become an essential global priority. In the energy sector, decarbonization and energy efficiency have to be pursued not only in electricity production, but also in mobility and heat production. Indeed, these sectors represent almost 60 % of final energy uses in Europe (Bellocchi *et al*., 2020) and, therefore, offer significant opportunities for improvement.
In particular, the electrification of heat generation through the use of heat pumps (HP), which are a well-known bridging technology between different sectors (Saletti *et al.*, 2023), is a promising alternative to fossil fuel-based conventional boilers (Gaur *et al*., 2020), as the heat demand of buildings is converted into an electricity demand. This, in turn, can be fulfilled by the power grid or by renewable energy sources (RES) such as wind and solar. Nevertheless, two issues in terms of power grid management arise from this electrification process. Firstly, the heat load of buildings is highly variable during the day, depending on the building thermal properties, external conditions and use (Verbeke and Audenaert, 2018), and is generally not synchronized with energy production from RES. This creates significant management challenges, often related to a peak load at the beginning of the day. Secondly, the thermal peak load of a large number of buildings, which become an electrical peak load when

https://doi.org/10.52202/077185-0138

fulfilled through HP, may overwhelm the capacity of the grid or lead to grid congestion (Fischer and Madani, 2017).

For these reasons, it is paramount to find flexibility measures on the demand side, as flexibility in production is not feasible due to RES penetration. A promising technique to pursue this target when supplying heat is known as Demand Side Management (DSM). One of the DSM approaches consists of actively using the thermal mass of buildings as thermal storage by changing the indoor temperature and, consequently, altering the profile of heat required (Guelpa and Verda, 2021). For instance, it is possible to store the heat generated by electricity (from RES or the grid) in the building and then exploit the stored heat to reduce the building heat demand in subsequent periods of the day.

There are different methods to regulate the heat supply in coordination with the thermal mass in a flexible way:

- Regulate the indoor temperature set-point over a given time window, with a negligible impact on user comfort;
- Change the control strategy of the conditioning system (Shi *et al.,* 2023): for instance activate or de-activate the HP to follow production from RES or a period of lower cost (Fambri *et al*., 2023), while ensuring comfort.

The former option is used when the origin of electricity is not well defined, and therefore it is not possible to distinctively determine the most profitable periods. The latter option, instead, is problem-dependent and has been investigated by several studies in the literature. Fambri *et al*. (2023) analyze the flexible use of HP for supplying heat to buildings while exploiting their thermal capacity as virtual energy storage, and they maximize the self-consumption of renewable electricity. The authors show that this method increased the self-consumed energy by up to 44 % without the need to install dedicated electrochemical storage. However, it is argued that the flexibility of buildings supplied by HP cannot be exploited during periods of low demand, when heat storage into the thermal mass could cause the indoor temperature to exceed the comfort level. Shi *et al.* (2023) state that there is not a unified method to quantify the performance of buildings as virtual energy storage. The authors propose instead charging and discharging time, and efficiency as performance indicators related to the building characteristics. As these parameters are evaluated on a specific building, they are case-dependent and cannot be used for a generic assessment of flexibility. Arteconi *et al*. (2019) suggest using four flexibility parameters combined within a flexibility performance index that rates buildings into different categories. Patteeuw *et al.* (2016) propose different types of incentives to load shifting, limiting the study to low-energy residential buildings and focusing on the electrical grid. Askeland *et al.* (2023) formulate the flexibility of space heating with a linear correlation between the energy stored and the indoor temperature increase, to facilitate its integration into linear optimization problems and also to aggregate several buildings. The authors remark the importance of reducing the number and complexity of building parameters that should be identified while using this procedure.

In this regard, the state-of-the-art research in building flexibility and DSM has mainly focused on detailed building models, for which significant challenges in tuning and parameter identification can be encountered. Additionally, the performance of the HP in terms of efficiency loss with varying load conditions is often neglected, providing a partial overview of the actual flexibility potential.

This paper aims to deal with these limitations by investigating the flexibility potential of an entire binary system comprising a building and a HP. The focus is the characterization of the binary system building-heat pump, with no regard to the source of electricity. This could be the power grid, with the scope of grid balancing, or a fluctuating renewable plant (be it photovoltaic or wind energy), with the aim of improving self-consumption, as well as another electricity production unit, for allowing its stable operation. Analyzing the binary system individually allows general considerations to be made, which can be implemented in all of the abovementioned cases. For this purpose, the system dynamic behavior is simulated through a model that requires a limited number of parameters, in order to foster generality and replication. The simulations are carried out by applying DSM strategies at different periods of the day and by varying the building thermal parameters. The flexibility potential is finally characterized through the evaluation of key performance indicators that represent the system dynamic response, electricity shift and HP performance. These data can be relevant in the definition of DSM strategies for entire communities.

https://doi.org/10.52202/077185-0138

2 SYSTEM MODEL

As confirmed by Arteconi *et al*. (2019), flexibility assessment in energy systems requires dynamic simulations. In fact, the dynamic behavior of a system in different situations and with diverse boundary conditions can be investigated by using mathematical models of the system, in which the parameters and characteristics of the system can be easily modified to assess their relevance to the results.
The model of a binary system building-heat pump is an assembly of components taken from a library developed by the authors and used in previous studies concerning energy systems of variable complexity, e.g. district heating networks (De Lorenzi *et al.*, 2020), energy hubs (Saletti *et al.*, 2022) and refrigeration plants (Di Mattia *et al*., 2022). The library is implemented in MATLAB®/Simulink®, a suitable environment for simulating dynamic systems. All components, as individual sub-systems, are modeled with a coherent causality to be able to construct complex systems in a modular way. The mathematical models of the library components, which span across energy domains such as the thermal, electrical and gas sectors, are based on the characterizing physical phenomena, represented by algebraic or differential equations. In this work, the library was enhanced with the inclusion of an additional component representing a HP, which was not available in the previous version (De Lorenzi *et al.*, 2020). While the general approach of the library is extensively described in the aforementioned papers, the description of the key components in the binary system is reported in the following sections to better illustrate the model. The binary system configuration is depicted in Figure 1.

2.1 Building model

A wide variety of research and commercial tools are available for simulating building dynamics, e.g. TRNSYS (Vadiee *et al*., 2019) and IDA ICE (Lundström *et al.*, 2019). Most of them require detailed knowledge on the building shape, structure and material composition. In studying flexibility, however, it is essential to find a compromise between the complexity and level of detail of information required about the system and the effort that has to be made to develop an appropriate model. Indeed, detailed building information is not always available or can often be imprecise, especially with old structures. Thus, constructing a precise model that has to be identified with imprecise or outdated details requires significant effort, which is not compensated by suitable performance. In addition, this engineering effort is even more relevant when large communities (i.e. many dwellings) are concerned.
For these reasons, this investigation relies on a simplified, but widely used, model of a single-zone building based on its energy conservation equation in differential form, as expressed in Eq. (1):

$$C_{\mathrm{b}}\frac{dT_{\mathrm{b}}}{dt} = -U_{\mathrm{b}}A_{\mathrm{b}}(T_{\mathrm{b}} - T_{\mathrm{ext}}) + \left(\dot{Q}_{\mathrm{b}} + \dot{Q}_{\mathrm{rad}} + \dot{Q}_{\mathrm{occ}}\right) - \dot{m}_{\mathrm{n}}c_{\mathrm{a}} \cdot (T_{\mathrm{b}} - T_{\mathrm{ext}}) - \dot{m}_{\mathrm{f}}c_{\mathrm{a}} \cdot (T_{\mathrm{b}} - T_{\mathrm{a}}) \qquad (1)$$

where T_{b} is the building indoor temperature and T_{ext} is the temperature of the external environment.

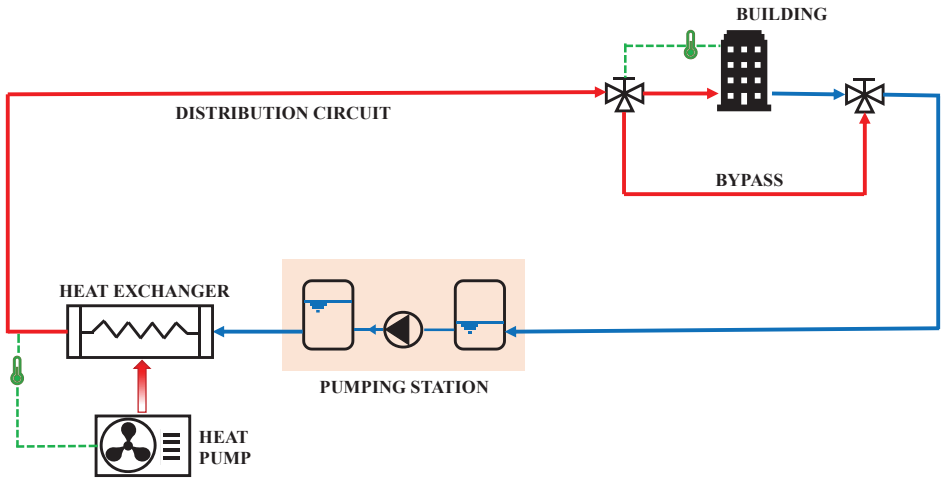

Figure 1: View of the university building taken as a case study.

https://doi.org/10.52202/077185-0138

C_b, U_b and A_b are the building total heat capacity (including air and envelope), heat transfer coefficient and exchange surface, respectively. The thermal power supplied to the building by the heating units, solar radiation and heat gains from the occupants of the dwelling are named $\dot{Q}_b$, $\dot{Q}_{rad}$ and $\dot{Q}_{occ}$, respectively. The air flow enters the sub-system through natural convection with rate $\dot{m}_n$ and through forced convection with mass flow rate $\dot{m}_f$ and temperature T_a (which depends on the potential heat recovered via the HVAC system), while its specific heat capacity is indicated by c_a.
It is possible to recognize four main contributions to the temperature dynamics, equal to the four addends: the heat lost through the building envelope, the heat obtained from external sources and the heat lost due to infiltration and forced ventilation. Eq. (1) is rearranged to express these contributions based on four performance coefficients that represent the overall behavior of the building, as in Eq. (2):

$$\frac{dT_b}{dt} = -a(T_b - T_{ext}) + b\left(\dot{Q}_b + \dot{Q}_{rad} + \dot{Q}_{occ}\right) - c(T_b - T_{ext}) - d(T_b - T_{air}) \quad (2)$$

The performance coefficients a, b, c and d are versatile parameters that can be calculated either from average material properties or from model identification starting from real or simulated data (Saletti *et al.*, 2020). An additional parameter that can be helpful in characterizing an individual building is its time constant, expressed by Eq. (3), since it gives an indication of the time required for the structure to cool down in the absence of an external load:

$$\tau = \frac{1}{a} = \frac{C_b}{U_b A_b} \quad (3)$$

The supplied thermal power $\dot{Q}_b$ is calculated as the heat exchanged between the water flowing within the heating units and the indoor air:

$$\dot{Q}_b = \dot{m}_w c_w (T_S - T_R) = UA\Delta T_{LM} \quad (4)$$

where $\dot{m}_w$ is the water mass flow rate sent to the building, c_w is the water specific heat capacity, while T_S and T_R are the supply and return water temperatures of the building heating units. In addition, UA and ΔT_{LM} represent the global heat transfer coefficient of the heating units and the logarithmic mean temperature difference between the inflowing water and the indoor air. Hence, it can be noted that the building model is coupled with the water distribution model (Section 2.3), as it receives the data of the water flowing in the circuit as inputs, according to the causality of the library.

2.2 Heat pump model

The heat pump is the bridging element between the electrical and thermal domains, as it is able to transfer heat from a low temperature source to a high temperature source thanks to the introduction of mechanical energy, supplied by an electric motor. Since they are designed to ensure comfort as standalone systems in the worst case scenarios, building heating units are often oversized. Therefore, they operate at partial load most of the time. There is good potential for using HP as flexibility providers, through regulating the heating parameters in coordination with the thermal capacity of the building envelopes and indoor air.
The heat $\dot{Q}_{HP}$ supplied to the high temperature source (i.e. the environment that has to be conditioned), is calculated with Eq. (5):

$$\dot{Q}_{HP} = COP \cdot P_{el} \quad (5)$$

where P_{el} is the electrical power that drives the motor and COP, known as Coefficient of Performance, is the representation of the conversion efficiency, which is strongly influenced by the load and temperatures of the two sources. According to international standard ISO 13612-2, the plant manufacturer declares the full-load COP (i.e. COP_{nom}) for different combinations of temperatures of the sources, which can be set in the sub-system by means of a user interface, together with other relevant characteristics. The actual COP_{nom} is therefore evaluated through a bilinear interpolation with the actual conditions of the sources, accounting for the second principle efficiency. Then, the downgrading of this

https://doi.org/10.52202/077185-0138

performance with the load is taken into account by calculating the Part Load Factor (PLF) given by Eq. (6):

$$PLF = \frac{COP}{COP_{\text{nom}}} = \left(1 - \frac{1-C_c}{PR}\right)\frac{1}{C_c} \quad (6)$$

where *PR* is the Power Ratio, namely the ratio between the actual electrical power P_{el} and the rated power of the HP, while C_c is a correction factor that considers the stand-by losses of the unit for an on/off operation. In absence of empirical data from the datasheets, this value is assumed as 0.9 (García-Céspedes *et al.*, 2020).

The newly developed HP model is an algebraic component based on the abovementioned equations, since its dynamics is significantly faster than the thermal dynamics of the building and water. It is valid for all kinds of HP, regardless of the heat sources. In particular, it can be applied also for Ground Source Heat Pumps (GSHP), in which the low-temperature source for withdrawal of heat is the soil. A specific sub-system provides the daily variation in soil temperature, which is, in any case, smaller than the variation in outdoor air temperature.

2.3 Distribution circuit model

The distribution circuit comprises the following components (Figure 1): a pumping station to allow the water to circulate, a supply pipeline, a return pipeline and a heat exchanger that receives the heat from the GSHP condenser.

The pumping station has a centrifugal pump and two expansion vessels that allow the water to expand during heating up and cooling down. The former is modeled through the algebraic characteristic curve of the machine. The curve calculates the water mass flow rate conveyed by the pump in the current operating conditions given by the pressure difference and the pump rotational speed. The expansion vessels are instead modeled through a physical approach, based on non-stationary mass and energy conservation equations applied to the gas volume contained within the vessel. In this way, the pressure of the water in the distribution system in the supply pipeline (downstream of the pump) and in the return pipeline (upstream of the pump) are evaluated. The pipeline model exploits the dynamic momentum and energy balance equations, including pressure and heat losses, to evaluate the outlet conditions of the water. In particular, the water that arrives at the building is carried within the supply pipeline, after receiving heat through the heat exchanger. This is a dynamic model that considers energy accumulation in the water contained in an equivalent pipe as well as equivalent pressure losses.

A three-way valve is present for allowing a part of the water mass flow rate to bypass the heating units within the buildings. While the pump is operated with a fixed rotational speed and, consequently, the total mass flow rate is also fixed, it is possible to set the valve opening in order to control the bypass flow rate. This may be necessary when the building indoor temperature is currently at a satisfactory value, and the thermal power supplied has to be lowered or disactivated. A second three-way valve allows the bypass flow and that sent to the building to be collected together after the component. Both valves are algebraic models represented by the mass and energy conservation equations.

3 SIMULATION SETUP

3.1 Description of the case study

The system considered is a simulated case study that collects the features of a university building located on the Campus of the University of Parma, in Italy, in order to simulate a realistic context (Figure 2). It is therefore an educational building with offices, classrooms and laboratories, a large heated surface (9500 m^2) and large areas of glazing. According to the Italian regulations for this end-use, the set-point for comfort temperature is 20 °C. Solar radiation, which is an input to the model, is rigorously calculated with a specific library block accounting for the time of year and relative position between the windows and the sun's rays. Internal gains, conversely, are estimated based on the opening schedule and number of users in the building throughout the days. The evolution over time of the external environment temperature derives from meteorological data for the specific area and time period.

The heat supply unit is a GSHP, the model of which is built with data from the manufacturer's datasheet. The soil is the low temperature source, while the high temperature source is assumed as the outlet temperature from the high temperature heat exchanger, which transfers heat from the GSHP working

https://doi.org/10.52202/077185-0138

fluid toward the building heating units. The water distribution circuit model is tuned starting from the geometrical characteristics (e.g. lengths and diameters of the pipelines) of the actual distribution network supplying the building. The main design parameters of the case study are reported in Table 1.

3.2 Control system

The control strategy of the binary system is a rule-based approach generally adopted in practice when such cases are concerned. The circulation pump of the circuit operates at constant rotational speed, determining a constant mass flow rate within the loop. The following three control logics are applied:

- The indoor temperature T_b is satisfied by a feedback controller that changes the opening of the three-way valve upstream of the user: the higher the error between the set-point and the actual T_b, the higher the portion of hot water sent to the building.
- The GSHP operation, in terms of electricity supplied to the unit, is modulated between the minimum PR, corresponding to an output heat ratio of 10 %, and 100 % of its nominal power (or turned off when necessary), in order to keep the water in the supply pipeline at a design temperature of 80 °C.
- An internal building controller varies the global heat transfer coefficient of the heating units (i.e. speed of thermal convectors) to maintain the return water at the design temperature.

3.3 Set of simulations

The flexibility of the described system is investigated by simulating its dynamic behavior when the indoor temperature of the building is modified, altering the desired set-point to maintain the occupants' comfort, for specific time windows at diverse periods of the day. To achieve this goal, a set of simulations for the same period of five days during winter is conducted, to reduce the influence of exogenous conditions on the results.

Figure 2: View of the university building taken as a case study.

Table 1: Main design parameters of the binary system building-heat pump.

Component	Parameter	Value	Unit
Building	Heat loss coefficient (a)	0.0201	h^{-1}
	Supplied power coefficient (b)	$1.7778 \cdot 10^{-7}$	°C kJ^{-1}
	Natural ventilation coefficient (c)	0.00896	h^{-1}
	Forced ventilation coefficient (d)	0.01943	h^{-1}
	Time constant (τ)	49.75	h
Heat pump	Nominal electrical power	450	kW
	Minimum Power Ratio	0.19	-
	COP_{nom} range of variation	2.38 to 3.73	-
Distribution circuit	Pipeline length	100	m
	Pipeline diameter	90	mm
	Nominal water mass flow rate	10	kg s^{-1}
	Nominal supply temperature	80	°C
	Nominal return temperature	60	°C

https://doi.org/10.52202/077185-0138

The parameters changed during these tests to characterize the flexibility of the binary system are as follows (Table 2):

- The indoor temperature set-point (fixed at 20 °C as baseline) is increased firstly to 20.5 °C, then to 21 °C for 4 hours, in order to store heat within the building. Such a time interval is selected to make sure DSM has a relevant effect and to obtain perceivable results. The simulations are repeated by scheduling the start of the time interval of set-point variation at all hours of the day. For instance, the first simulation contains a set-point variation from 00:00 to 04:00, the second from 01:00 to 05:00, and so on, until the last simulation has a variation from 23:00 to 03:00 of the following day.
- The time constant of the building is changed in order to verify if the results can be transferred to binary systems with a different thermal response, and if generic rules can be drawn.
- A condition with the correction coefficient C_c of the GSHP equal to 1, indicating that the COP is not subject to downgrading with the load, is tested as a benchmark for comparison.

The results of the simulations are analyzed from the second day on, in order to reject the influence of the initial numerical transient. Since all sub-systems are modeled with a physics-based approach, it is possible to monitor all relevant physical variables in the simulation platform, e.g. electrical power, thermal power, mass flow rates, temperatures of the building and water in the distribution circuit, and valve opening. The relevant variables can be post-processed to calculate indicators of flexibility, as explained in the following section.

3.4 Key Performance Indicators

The numerical results of the set of simulations listed in Section 3.3 are compared with the respective reference simulations, expressed with the subscript "base" in which no parameter is altered. In particular, the indoor set-point is kept at 20 °C and the binary system flexibility is not explicitly utilized. The Key Performance Indicators (KPI) that are used to quantify the different management of the binary system in the presence of a changed parameter are reported in Table 3. The KPI pertain to the variation of electricity E_{el} used by the GSHP compared to the reference (preheating the building during the set-point variation, but also discharging it afterwards), to the variation of heat E_{th} produced, to the discharge time, and to a combination of these elements. In more detail, The last KPI R_E represents the increase in electricity divided by the average heating degree-hours of the discharge period. It gives an indication of how much electricity can be stored, in the form of heat, within the building mass with respect to the average requirement for heating during the discharge phase.

4 RESULTS

The results of the complete set of simulations conducted to evaluate the flexibility potential of the binary system building-heat pump mentioned in Section 3.3, are discussed in the light of the KPI listed in Table 3. In particular, it is of key interest to compare the evolution of the electrical power fed to the GSHP over time in the different cases. This would enable the possibility to dynamically move a portion of the electricity request, in order to follow a period of lower electricity cost or to provide a flexibility or balancing service to the power grid.

Table 2: Set of simulations for investigating the flexibility of the binary system.

Number of simulations	Set-point variation	Time constant variation	C_c of the GSHP	Schedule
1	-	-	0.9	Reference with set-point at 20 °C
24	+0.5 °C	-	0.9	Time interval of 4 hours starting from midnight (1st simulation) to 23:00 (24th simulation)
24	+1.0 °C	-	0.9	All set-point temperature variations
24	+1.0 °C	-	1	All set-point temperature variations
24	+1.0 °C	-20 %	0.9	All set-point temperature variations
24	+1.0 °C	+20 %	0.9	All set-point temperature variations

https://doi.org/10.52202/077185-0138

Table 3: Definition of Key Performance Indicators for characterizing the flexibility of the binary system. *E* is the electricity used to power the HP (subscript el) or the heat produced (subscript th).

KPI	Formulation	Unit	Description
Increased E	$E^{+} = E - E_{\mathrm{base}}$	kWh	Increase in electricity use or heat produced during four hours of set-point variation
Reduced E	$E^{-} = E_{\mathrm{base}} - E$	kWh	Reduction in electricity use or heat produced during remaining 20 hours after variation
Discharge time	τ_{dis}	h	Time between end of set-point variation and reactivation of heating
Dimensionless discharge time	$R_{\tau} = \frac{\tau_{\mathrm{dis}}}{\tau}$	-	Ratio between discharge time and building time constant
Increased E per average degree-hour	$R_{E} = \frac{E_{\mathrm{el}}^{+}}{\left(T_{\mathrm{SP}} - T_{\mathrm{ext,avg}}\right)}$	kWh/°C	Increased E per average heating degree-hour during discharge time

In this regard, the GSHP operation in the reference case (i.e. indoor temperature set-point is fixed at 20 °C) and with an increase of 1 °C during two different sets of four hours is represented in Figure 3. The selected results are for a set-point variation scheduled during the night (from 01:00 to 05:00) and then during the morning (from 08:00 to 12:00). Although the simulations involve five days in January, it is remarked that the results of the first and last days are omitted to reduce the influence of transient conditions. In both the depicted cases, the sharp increase in electric power to the GSHP can be noted during the four-hour set-point variation. However, during the night variation, the GSHP is operated at full load for the entire period of four hours while, during the morning variation, this happens for a limited time (i.e. around two hours in this specific case).

This can be explained by looking at Figure 4, which shows the indoor building temperature realized in the same conditions. When a set-point variation is scheduled during the night, the new desired temperature of 21 °C is not reached, despite the heating units operating at its nominal load, while in the morning case, the steady-state at the new set-point is reached before the end of the variation. Moreover, this is due to a twofold effect. On the one hand, during the night the lower outdoor temperature forces the heating unit to contrast higher heat dispersion from the building envelope. On the other hand, since the night load is already higher than the day load in the reference case, the power increase allowed with respect to the reference is much lower during the night, due to the saturation of the GSHP load to its nominal value, as clearly visible from Figure 3. Afterwards, the GSHP is also completely turned off for different periods of time, while waiting for the building to cool down to 20 °C at different speeds, depending on the outdoor conditions and contribution of the internal gains (e.g. daily occupation).

In addition, it can be observed that a morning variation (from 08:00 to 12:00) prevents the GSHP from operating in a discontinuous way at low heat loads, due to the limit on minimum load (i.e. 10% of the heating nominal value). The discontinuous operation is instead maintained when the variation is scheduled at night, since periods of low load persist.

The effects shown in this work are further confirmed by the comparison with other literature studies. For instance, the GSHP production profile depicted in Figure 3 resembles that reported by Fambri *et al*. (2023). It is however essential to show the results obtained for all schedules of set-point variations at 21 °C, in order to identify possible trends of the KPI when DSM is applied at different times. Figure 5 shows the increased electricity E_{el}^{+} and reduced electricity E_{el}^{-}, for each day and schedule, while Figure 6 illustrates the overall electricity variation throughout the day, compared to the reference. Firstly, it can be noted that the increased electricity, stored within the building thermal mass in the form of heat when the set-point is increased, is always lower than the electricity that is not used during the remaining portion of the day. This leads to overall electricity savings between 1 % and 5 %, with a higher overall reduction when the set-point change is scheduled for the early morning (i.e. between 04:00 and 07:00). This conclusion could appear controversial, as it seems to be possible to retrieve more electricity than that stored previously within the building. Nevertheless, it can be explained by the different operating rates of the GSHP shown in Figure 3, and by remarking that the energy vector that is effectively stored is heat.

https://doi.org/10.52202/077185-0138

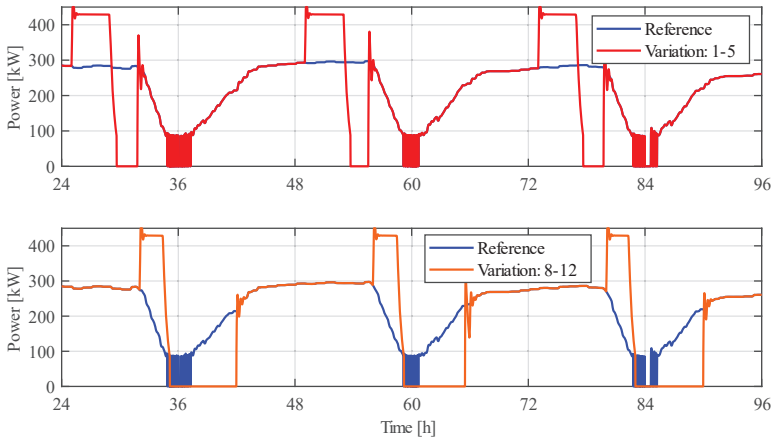

Figure 3: Electricity supplied during the three central days of the simulation. Comparison between the reference (set-point at 20 °C) and a set-point variation at 21 °C for two different time schedules.

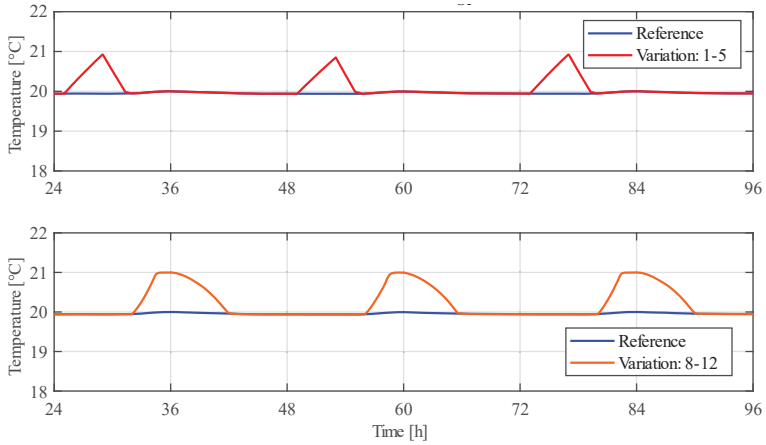

Figure 4: Building temperature during the three central days of the simulation. Comparison between the reference (set-point at 20 °C) and a set-point variation at 21 °C for two different time schedules.

When the set-point is increased, the GSHP operates at full load, with the highest COP for the given set of source temperatures, instead of operating with lower performance as in the reference. Consequently, it is possible to store a given amount of heat with a low electricity expense. In addition, the same amount of heat (net of heat losses) is retrieved while the structure cools down to 20 °C. This is related to the time period in which the GSHP would operate at low performance and with a relatively high electricity expense, which is instead avoided.

Another interesting effect regards the amount of electricity that can be shifted, which is slightly lower when the DSM happens during the night. Again, this appears to be an anomalous behavior, but it is justified by the saturation effect of the GSHP load. As commented above, the power difference between the full load and reference is lower during the night and late evening, reducing the amount of additional electricity that can be transferred during the four hours of set-point change.

Figure 7 shows the discharge time, which is subject to a large oscillation and presents a symmetrical behavior to the electricity variation. The GSHP can be completely turned off from 2 h to almost 8 h, hence ranging from 4 % to 16 % of the building time constant. Once more, the discharge time is remarkable when the set-point variation is planned in the early morning, between 04:00 and 09:00, probably due to the possibility to take advantage of additional gains from the building occupants and radiation, and slow down the period of discharge to 20 °C. Finally, it can be stated that these indicators are not considerably influenced by the specific day, but more by the period of the day in which the change is scheduled.

https://doi.org/10.52202/077185-0138

The results described above are valid for the simulation with a set-point increase by 1 °C, and aim to show the sensitivity of the key variables when this variation is scheduled at different periods of the day. Table 4 lists instead the complete set of results obtained by monitoring the KPI in all simulations. The range shown is valid for three central days and for all set-point variation times. For the trends at the different times, it is sufficient to refer to the previous figures.

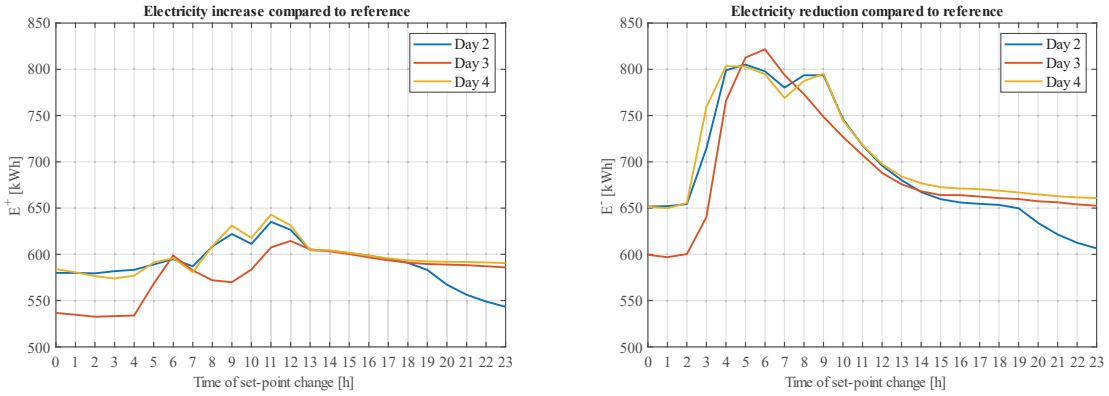

Figure 5: Daily electricity increase (left) and daily electricity reduction (right) compared to the reference, depending on the starting hour of the set-point variation at 21 °C.

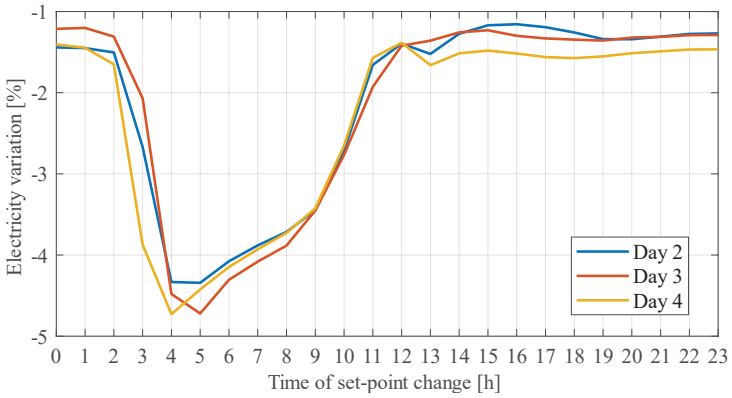

Figure 6: Percentage variation of electricity consumed daily compared to the reference, depending on the starting hour of the set-point variation at 21 °C.

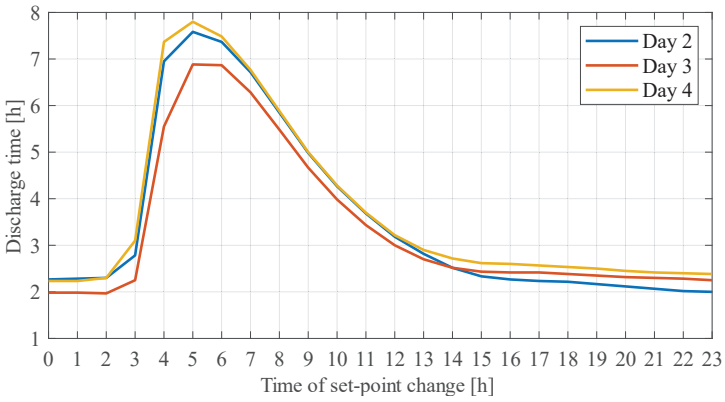

Figure 7: Discharge time depending on the starting hour of the set-point variation at 21 °C.

https://doi.org/10.52202/077185-0138

Table 4: Range of values of Key Performance Indicators for the different simulation sets.

KPI	SP: +0.5 °C C_c = 0.9	SP: +1.0 °C C_c = 0.9	SP: +1.0 °C C_c = 1	SP: +1.0 °C τ: -20 %	SP: +1.0 °C τ: +20 %
E_{el}^{+} [kWh]	260 to 308	532 to 643	591 to 730	461 to 515	533 to 767
E_{el}^{-} [kWh]	323 to 468	597 to 822	575 to 662	518 to 678	603 to 952
$\frac{E_{el}^{+}-E_{el}^{-}}{E_{el,base}}$ [-]	-3.27 to -0.54	-4.73 to -1.16	0.28 to 1.75	-3.87 to -0.71	-5.20 to -1.32
E_{el}^{-}/E_{el}^{+} [-]	1.08 to 1.57	1.10 to 1.43	0.89 to 0.98	1.07 to 1.42	1.11 to1.46
E_{th}^{-}/E_{th}^{+} [-]	0.87 to 0.93	0.86 to 0.94	0.86 to 0.95	0.84 to 0.92	0.88 to 0.95
τ_{dis} [h]	1.02 to 5.7	1.97 to 7.8	1.97 to 7.8	1.73 to 7.07	1.97 to 8.07
R_τ [-]	0.02 to 0.11	0.04 to 0.16	0.04 to 0.16	0.04 to 0.18	0.03 to 0.14
R_E [kWh °C^{-1}]	13.4 to 16.5	27.1 to 34.5	30.1 to 39.4	23.5 to 27.6	27.1 to 41.2

It emerges that:

- The electricity that can be shifted drops to around half when the set-point increase is 0.5 °C, instead of 1 °C, suggesting a linear correlation. The same is seen with the time constant.
- The ratio between the increased and reduced heat from the GSHP is similar in all cases, regardless of the value of the DSM applied and of the building time constant. The same happens to the ratio between increased and reduced electricity, except when the GSHP efficiency downgrading is not accounted for (C_c equal to 1). This is the only case in which the overall electricity consumption increases, as the different GSHP rates cannot be exploited. The consumption is higher because the increase in indoor temperature determines higher heat losses through the envelope.
- The dimensionless discharge time is slightly reduced with an increase in the time constant, as the higher building capacity is not counterbalanced by an equivalent increase in discharge time.
- The shifted electricity per average degree-hour ranges from 27 kWh/°C to 41 kWh/°C, but it drops to (13.4 to 16.5) kWh/°C when the set-point increase is halved.

While appearing promising for implementing DSM in binary systems, it has to be underlined that these general considerations derive from the assumption that the indoor comfort is the same all day. The results may differ when a night set-back temperature is applied. This, however, would impose a significant peak load at the beginning of the day, which could hinder the implementation of DSM. Furthermore, the COP variation of the GSHP may differ from that used in this work (declared valid mainly for on-off HP) when HP with inverters are involved. In any case, the presented methodology, which proved effective, will be further employed to examine and cover these limitations.

5 CONCLUSIONS

This work presented a methodology to characterize the flexibility inherent in binary systems of buildings and heat pumps, in order to implement heat demand side management and shift the deriving electrical load. A model that considers building and distribution network dynamics was used to perform a set of simulations in which the indoor temperature set-point is increased with moving time windows of four hours. It was shown that an increase in the temperature set-point at strategic parts of the day (i.e. early morning) can determine remarkable discharge times and electricity savings up to 5 % by allowing the heating unit to avoid part load operation. The most determinant effects were the consideration of the heat pump performance downgrading with the load, and the possibility to benefit from the internal gains to extend the building discharge period. It was also found that the electricity that can be shifted with respect to the heating degree hours ranges from 27 kWh/°C to 41 kWh/°C when the set-point is increased by 1 °C. The analysis of these indicators can open up new management opportunities in communities of buildings. Indeed, once all binary systems in a community are characterized, it is possible to coordinate them to achieve energy efficiency goals, such as minimal energy use or minimal cost. As a future perspective, the knowledge acquired in this work can be incorporated into digital management tools that can autonomously exploit flexibility in communities of buildings and put efficiency goals into practice.

https://doi.org/10.52202/077185-0138

REFERENCES

Arteconi, A., Mugnini, A., Polonara, F., 2019, Energy flexible buildings: A methodology for rating the flexibility performance of buildings with electric heating and cooling systems, *Appl. Energy*, vol. 251, 113387.

Askeland, M., Georges, L., Korpås, M., 2023, Low-parameter linear model to activate the flexibility of the building thermal mass in energy system optimization, *Smart Energy*, vol. 9, 100094.

Bellocchi, S., Manno, M., Noussan, M., Prina, M. G., Vellini, M., 2020, Electrification of transport and residential heating sectors in support of renewable penetration: Scenarios for the Italian energy system, *Energy*, vol. 196, 117062.

De Lorenzi, A., Gambarotta, A., Morini, M., Rossi, M., Saletti, C., 2020, Setup and testing of smart controllers for small-scale district heating networks: An integrated framework, *Energy*, vol. 205, 118054.

Di Mattia, E., Gambarotta, A., Marzi, E., Morini, M., Saletti, C., 2022, Predictive Controller for Refrigeration Systems Aimed to Electrical Load Shifting and Energy Storage, *Energies*, vol. 15(19), 7125.

Fambri, G., Marocco, P., Badami, M., Tsagkrasoulis, D., 2023, The flexibility of virtual energy storage based on the thermal inertia of buildings in renewable energy communities: A techno-economic analysis and comparison with the electric battery solution, *J. Energy Storage*, vol. 73, 109083.

Fischer, D., Madani, H., 2017, On heat pumps in smart grids: A review, *Renew. Sustain. Energy Rev.*, vol. 70, 342-357.

García-Céspedes, J., Arnó, G., Herms, I., De Felipe, J. J, 2020, Characterisation of efficiency losses in ground source heat pump systems equipped with a double parallel stage: A case study, *Renew. Energy*, vol. 147, 2761-2773.

Gaur, A. S., Fitiwi, D. Z., Curtis, J., 2021, Heat pumps and our low-carbon future: A comprehensive review, *Energy Res. Soc. Sci.*, vol. 71, 101764.

Guelpa, E., Verda, V., 2021, Demand response and other demand side management techniques for district heating: A review, *Energy*, vol. 219, 119440.

Lundström, L., Akander, J., Zambrano, J., 2019, Development of a space heating model suitable for the automated model generation of existing multifamily buildings—a case study in Nordic climate. *Energies*, vol. 12(3), 485.

Patteeuw, D., Henze, G. P., Helsen, L., 2016, Comparison of load shifting incentives for low-energy buildings with heat pumps to attain grid flexibility benefits., *Appl. Energy*, vol. 167, 80-92.

Saletti, C., Gambarotta, A., Morini, M., 2020, Development, analysis and application of a predictive controller to a small-scale district heating system, *Appl. Therm. Eng.*, vol. 165, 114558.

Saletti, C., Morini, M., Gambarotta, A., 2022, Smart management of integrated energy systems through co-optimization with long and short horizons, *Energy*, vol. 250, 123748.

Saletti, C., Morini, M., Gambarotta, A., 2023, Smart Management for Integrated Energy Systems: Tools from Communities to Regions., *36th International Conference on Efficiency, Cost, Optimization, Simulation and Environmental Impact of Energy Systems (ECOS 2023),* pp. 3374-3385.

Shi, W., Liu, Q., Ruan, Y., Qian, F., Meng, H., 2023, Quantification and economic analysis of virtual energy storage caused by thermal inertia in buildings, *Journal of Physics: Conference Series* , vol. 2474, No. 1, p. 012002, IOP Publishing.

Vadiee, A., Dodoo, A., Jalilzadehazhari, E., 2019, Heat supply comparison in a single-family house with radiator and floor heating systems, *Buildings*, vol. 10(1), 5.

Verbeke, S., Audenaert, A., 2018, Thermal inertia in buildings: A review of impacts across climate and building use, *Renew. Sustain. Energy Rev.*, vol. 82, 2300-2318.

ACKNOWLEDGEMENT

This work was co-authored by a researcher with a research contract co-funded by the European Union – PON Ricerca e Innovazione 2014-2020 (according to Italian legislation: art. 24, comma 3, lett. a), della Legge 30 dicembre 2010, n. 240 e s.m.i. e del D.M. 10 agosto 2021 n. 1062).

https://doi.org/10.52202/077185-0138